Gearbox fault detection using a new denoising method based on ensemble empirical mode decomposition and FFT

Hafida MAHGOUN[1], Rais.Elhadi BEKKA[2] and Ahmed FELKAOUI[1]

[1]Laboratory of applied precision mechanics (LMPA), Institute of optics and precision mechanics.
University Ferhat Abbas, Sétif1,19000 Algeria
[2]Institute of electronic
University Ferhat Abbas, Sétif1, 19000 Algeria
{mahafida006}@yahoo.fr

Abstract

The vibration signal of a gearbox carries important information which can be used in early damage detection and fault diagnosis, however this signal is usually noisy and the information about the fault in the early stage of its development can be lost. Ensemble Empirical Mode Decomposition (*EEMD*) is a new method and a powerful tool in signal processing. In this paper, a de-noising technique based on ensemble empirical mode decomposition and fast Fourier transform (*FFT*) is used to post processing the noisy vibration signal taken from a test bench. Firstly, the signal is decomposed into a number of *IMF*s using the *EEMD* decomposition. Secondly, the denoising method based on the thersholding of Donoho and *FFT* is applied to IMFs to remove the noise. To detect the damage at an early stage a statistical method based on Kurtosis is used. The different stages of the technique, which is named (*DEEMDFFT*), are introduced in detail. The results given by this technique are compared to those given by wavelet transform (*WT*) by using simulated and experimental signals.

1 Introduction

Vibration signals are widely used in rotating machines faults diagnosis and precisely in gearboxes fault detection. These signals carry important information which is very useful in early detection of defect [1],[2]. Many techniques have been proposed for processing vibration signals [3]-[8]. The time-frequency analysis methods can provide both time and frequency information of signal [9]. Particularly the Short Time Fourier Transform (STFT) [6], Wigner-Ville distribution (WVD) [5] and Wavelet Transform (WT) [7] are widely used in gearbox diagnosis. However, these techniques present some limits and drawbacks. The STFT is appropriate to analyzing the signals with slowly varying [9] and it is inefficient for the analysis of non-stationary signals such the gearbox vibration signals. The WVD method suffers from the cross terms as by indicated the existence of negative energy for some frequency ranges and from the aliasing problem [9]. The use of pseudo WVD eliminates negative power and therefore also the aliasing problem. However, the results obtained with pseudo WVD can be difficult to interpret [10]. The limitations of STFT and WVD can be overcome by using the WT [11]. However the main drawback of the WT is the difficulty of choosing wavelet base function and the number of levels [7], [12]. To avoid the disadvantage of the choice of wavelet basis function, empirical mode decomposition (EMD) was originally proposed by Huang et al. [13]-[14] for nonlinear and non-stationary signals and was recently applied in fault diagnosis of rotating machinery [12], [15]-[17]. The EMD does not use a priori determined basis functions and can iteratively decompose a complex signal into a finite number of intrinsic mode functions (IMFs). Each resulting elementary component IMF can represent the local characteristic of the signal. However, EMD method cannot sometimes reveal the signal characteristics correctly due to the mode mixing effect [18]. Mode mixing shows that oscillations of different time scales reside in a given IMF or oscillation of the same time scale exits in different IMFs. To prevent the problem of mode mixing in EMD, the ensemble empirical mode decomposition (EEMD) was used recently [19]-[20]. The principle of the EEMD is based on the addition of the white noise in the signal with many trials. The noise in each trial is different. The EEMD method defines the IMF components as the mean of an ensemble of trials. On the other hand,

the measured signal is contaminated by noise, which can be generated by different sources, as the hardware employed during data collection. Then the presence of noise may increase the amplitude noise used by EEMD which increases the EEMD error and decreases the accuracy of the IMFs. In that case, the use of this technique alone may display low sensitivity to faults detection, precisely in the early stage of their development [20]. In this work, we present a new method to denoise the vibration signals by the EEMD in purpose to analyze the gearbox data. Firstly, the gearbox signal is decomposed into a collection of IMFs by the EEMD, next, the coefficient of correlation (coefcor) between the signal and each IMF is calculated, the IMF which the coefcor is less than 0.1 was eliminated because it considered as a noise, after that, a de-noising method based on thersholding [21] and FFT are applied to de-noise the noisy IMFs. Finally, the signal is reconstructed using the denoised IMFs. The main advantages of this procedure are that no artificialinformation is introduced into the de-noised signal and the IMFs are independently threshold. The results obtained by this method are compared to those obtained by using wavelets. In this paper we have also used Kurtosis as indicator to extract periodic impulses due to defects. Simulation signal was initially used to evaluate the performance of this new de-noising method. Experimental results show that the noise contaminating the gearbox signal was considerably removed and the defect has been detected at very early stage compared to the results given in the literature. The structure of the paper is as follows: section 2 introduces the basic of EMD and EEMD methods. Section 3 presents the procedure of the denoising method based on EEMD. In section 4, we present a simulated signal to illustrate the behavior of the algorithm proposed then in section 5 the method is applied for gearbox faults diagnosis. In section 6, a conclusion of this paper is given.

2 EMD and EEMD Algorithms

2.1 EMD algorithm

The EMD consists to decompose iteratively a complex signal into a finite number of intrinsic mode functions (IMFs) which verify the two following conditions:

1. the number of extrema and the number of zeros of an IMF must be equal or differ at most by one,
2. an IMF must be symmetric with respect to local zero mean.

For a given signal $x(t)$ the EMD algorithm used in this study is summarised as follows [13]-[14]:

1. Identify the local maxima and minima of the signal $x(t)$
2. Generate the upper $x_{up}(t)$ and lower envelops $x_{low}(t)$ of $x(t)$ by the cubic spline interpolation of the all local maxima and the all local minima.
3. Average the upper and lower envelops of $x(t)$ to obtain the local mean function:

$$m(t) = \frac{x_{up}(t) + x_{low}(t)}{2} \tag{1}$$

4. Calculate the difference

$$d(t) = x(t) - m(t) \tag{2}$$

   If $d(t)$ verifies the above two conditions, then it is an IMF
5. replace $x(t)$ with the residual $r(t) = x(t) - d(t)$ otherwise, replace $x(t)$ with $d(t)$

   Repeat steps (1)-(5) until the residual satisfies the criterion of a monotonic function. At the end of this algorithm, the signal can be expressed as:

$$x(t) = \sum_{n=1}^{N} c_n(t) + r_N(t) \tag{3}$$

   where $c_n(t)$ are IMFs, N is the number of IMFs extracted named and $r_N(t)$ is the final residue.

2.2 EEMD algorithm

To alleviate the mode mixing effect of EMD, the EEMD was used. The EEMD decomposition algorithm of the original signal used in this work is summarised in the following steps [19]:

1. Add a white noise with given amplitude to the original signal to generate a new signal:

$$x_k(t) = x(t) + \beta_k n(t) \tag{4}$$

2. Use the EMD to decompose the generated signals $x_k(t)$ into N IMFs

$$c_{nk}(t), n = 1, \cdots, N \tag{5}$$

where $c_{nk}(t)$ is the nth IMF of the kth trial.

3. Repeat steps (1) and (2) K times with different white noise series each time to obtain an ensemble of IMFs:

$$c_{nk}(t), k = 1, \cdots, K \tag{6}$$

4. Determine the ensemble mean of the K trials for each IMF as the final result:

$$c_n(t) = \lim_{K\to\infty} \frac{1}{K} \sum_{k=1}^{K} c_{nk}(t), n = 1, \cdots, N \tag{7}$$

The relationship among the amplitude of the added white noise and the number of ensemble trials is given by [19]:

$$\delta_k = \frac{\beta_k}{\sqrt{K}} \tag{8}$$

where K is the number of ensemble trials, is the amplitude of the added noise and is the corresponding IMF(s). The results given by EEMD are strongly influenced by the choice of the sampling frequency [22].

3 Fourier Transform Threshold de-noising

Let $y(t)$ be a clean signal corrupted by an additive white Gaussian noise $b(t)$ as follows:

$$\mathrm{x(t)} = \mathrm{y(t)} + \mathrm{b(t)} \tag{9}$$

The aim of denoising technique is to recover an approximation $\tilde{\mathrm{y}}(\mathrm{t})$ as closely as possible to the original clean signal $y(t)$ in order to eliminate noise components. The most famous denoising approach is wavelet thresholding, the fundamental reasoning of wavelet thresholding is to set to zero all the components that are lower than a threshold related to the noise level, and then reconstruct the denoised signal utilizing the high-amplitude components only. The three steps of de-noising used to denoise a signal using FFT are:

1. Apply fast Fourier transform (FFT) to noisy signal,
2. Revise the FFT coefficients with the threshold operator,
3. Perform inverse fast Fourier transform (IFFT) to obtain the denoised signal.

By using EEMD the noisy signal is expressed as:

$$x(t) = \sum_{n=1}^{N} c_n(t) + r_N(t) \tag{10}$$

The extracted IMFs include the noise since each IMF, indexed by n, can be approximated as follows:

$$c_n(t) = cc_n(t) + b_n(t) \tag{11}$$

where: $cc_n(t)$: is the noiseless IMF. When we applied the FFT to each IMF we get C_{ni} coefficients and the two classical thresholding functions hard thresholding and soft thresholding can be used. The hard thresholding estimator can be expressed as:

$$C_{ninew} = \begin{cases} C_{niold} & if \ |C_{ni}| > TH \\ 0 & if \ |C_{ni}| \leq TH \end{cases} \tag{12}$$

The soft thresholding estimator decreases the amplitude of all noisy coefficients. The soft thresholding function is can be expressed as:

$$C_{ninew} = \begin{cases} sign\,(C_{niold})\ (|C_{niold} - TH|) & if \ |C_{ni}| > TH \\ 0 & if \ |C_{ni}| \leq TH \end{cases} \tag{13}$$

Donoho [21]gave the uniform threshold in equation (14) that can be applied in the hard and soft thresholding:

$$\mathrm{TH} = \sigma\sqrt{2\,\log(l)/l} \tag{14}$$

In this study l is the length of the IMF, and σ : is the noise variance and can be estimated by

$$\tilde{\sigma} = \mathrm{MAD}/0.6754 \tag{15}$$

MAD is the median of the absolute deviation value. The main purpose of de-noising step is to suppress the component representing noise and to regain the cc̃ as the estimate of the noiseless IMF. And finally, the estimated signal,$\tilde{y}(t)$ is given by :

$$\tilde{y}(t) = \sum_{n=1}^{N} c\tilde{c}_n(t) + r_N(t) \tag{16}$$

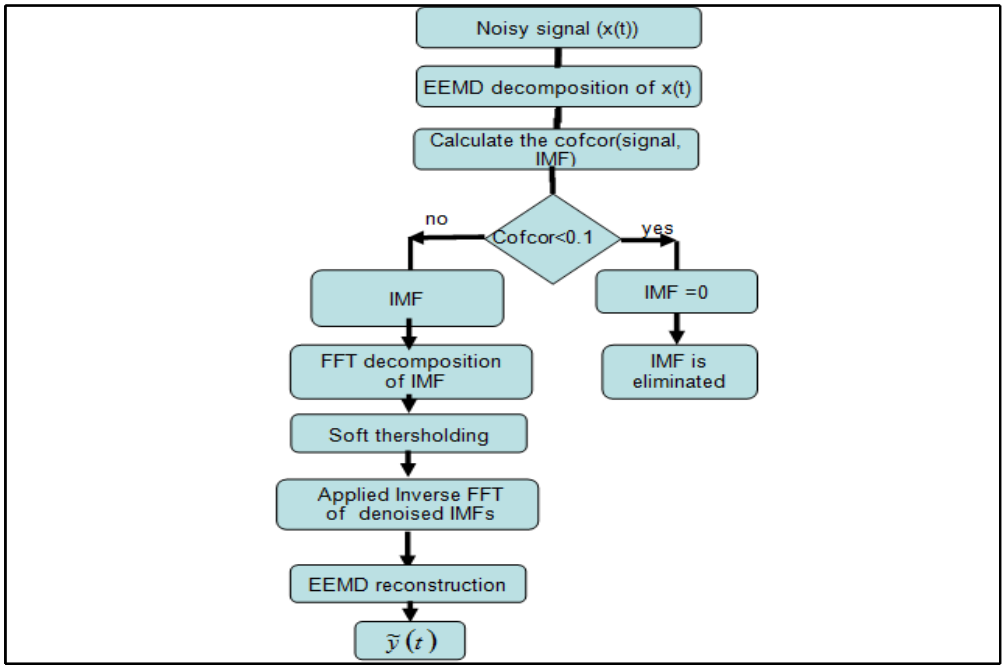

Figure 1: Diagram of EEMD FFT denoising.

4 Simulation

Consider a signal , which involves two sin components of $50Hz$ and $100Hz$, as defined below:

$$y\,(\mathrm{t}) = \sin(2\pi.120.t) + \sin(2\pi.50.t) \tag{17}$$

Fig.2 shows the multicomponent signal. By using the EEMD, the signal is decomposed into two IMFs and a residue. Fig.3 gives the signal IMFs and the residue. The first IMF illustrates the harmonic components of sin of 120Hz, and the second IMF illustrates the harmonic components of sin of 50Hz, the residue is nearly zero vectors. In practice, it is sure that noise will be introduced into the vibration signal. If we take the same signal and introduced a white noise Fig.4.

$$\mathrm{x}\,(\mathrm{t}) = \sin(2\pi.120.t) + \sin(2\pi.50.t) + noise(t) \tag{18}$$

The EEMD results of $x(t)$ are shown in Fig.5, the figure demonstrates that the signal is over decomposes because the noise introduce some false local extrema and the sampling frequency is 20000Hz, we have taken a very large sampling frequency to get many IMFs which represent only the noise. Table.1 gives the coefficients of correlation between the signal and each IMF. The first three IMFs were eliminated because their coefficients of correlation are less than 0.1. In order to remove the noise from the IMFs, we have applied two different methods, the first method is the de-noised method based on FFT (Fig.6) and the second method is based on wavelet transform (WT), and we have compared between results given by the two methods (Fig.7), we can see clearly that FFT gives best results. Fig.8 shows the zoom of the de-noised signal given in figure 7 . In order to control the error and the level of noise, we have calculated the mean square error (MSE) between the noiseless signal and the denoised signal and the values of signal to noise ratio (SNR) after denoising. The results given by DEEMDFFT method were compared to the results given by WT (Table.2). MSE is given by :

$$\mathrm{MSE} = \sqrt{\sum (\tilde{\mathrm{y}}\,(\mathrm{t}) - y\,(t))^2 \Big/ T} \tag{19}$$

The SNR before denoising is given by:

$$\mathrm{SNR} = 10\log \frac{\sum\limits_i y_i^2}{\sum\limits_i b_i^2} \tag{20}$$

The SNR after denoising is given by:

$$\mathrm{SNR} = 10\log \frac{\sum\limits_i y_i^2}{\sum\limits_i (y_i - \tilde{y}_i)^2} \tag{21}$$

where,$y(t)$: is the noiseless signal, $\tilde{y}(t)$: is the denoised signal and $b(t)$: is the noise.

IMF1	IMF2	IMF3	IMF4	IMF5	Res
0.056	0.035	0.53	0.77	0.71	0.16

Table 1: Coefficient of correlation $(x(t), IMFs)$

SNR (dB) before denoising	Denoised signal (WT)		Denoised signal (EEMDFFT)	
	SNR(dB)	MSE	SNR(dB)	MSE
20	28.58	4.15	29.22	3.58
10	20.88	24.45	21.62	20.65
5	15	99.5	17.92	48.39

Table 2: Comparison between wavelets and the proposed method

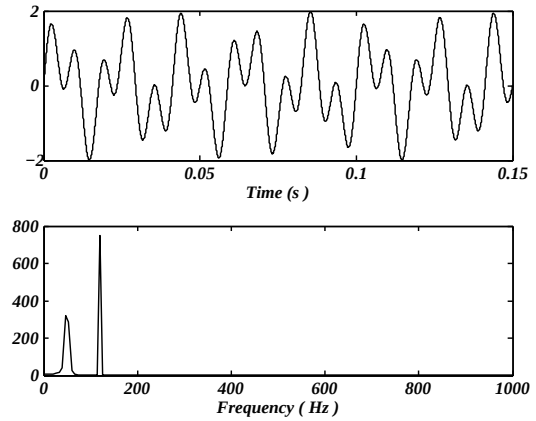

Figure 2: The simulated signal(noisless), a) the time domain, b) the spectrum.

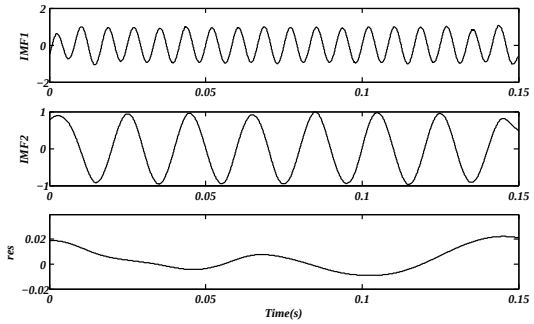

Figure 3: EEMD decomposition of the simulated signal.

5 Application to experimental data

The vibration signals used in this work were carried out at CETIM, France [23]. The system under test is composed of a pair of spur gears which have a number of teeth respectively $Z1 = 20\ teeth$ and $Z2 = 21\ teeth$, the 20 $teeth$ gear has a rotation speed of 1000 rpm. The experiment was carried out for $13 days$ length and the measurements were collected every $24h$, on the last day the fault was in an advanced stage close to the breakage of the tooth. The rotating speed of the input shaft is : $fr1 = 16.67\ Hz$ and the rotating speed of the output shaft is $fr2 = 15.87\ Hz$ the meshing frequency is $fe = Z1.fr1 = Z2.fr2$ then it is $fe = 333\ Hz$, Fig.9 shows the acceleration signals in time domain; they correspond to five days of the experiment "$2^{nd}day, 6^{th}day, 9^{th}day, 11^{th}day$ and $13^{th}day$". The time trend of the vibration signals corresponding to $2^{nd}day, 6^{th}day, 9^{th}dayand 11^{th}$ day indicate that it is not possible to detect the fault of the gear only by looking at the time trend plot since impulses due to faults are masked by the noise. For the vibration signals corresponding to the last day 13^{th}, we can see that the fault is characterized by periodical impulses caused by cracked teeth. Then the fault is in advanced stage. Table. 3 gives the expert report, we note that for the first day there is no acquisition of data. Our purpose is to identify the fault from the collected vibration signals before the tooth was broken. In this section, first we have calculated the kurtosis values for acceleration signals from day 2 to 13, and then each signal was decomposed by the EEMD method, we have obtained 12 IMFs which are reduced to (4 or 5) IMFs, because we have taken only the IMFs of which their coefficient of correlation with the signal is greater than 0.1, (Figure.10 and Figure.11) show the EEMD results for 2nd day and last day. Then, every IMF was decomposed using Fast Fourier Transform (FFT), and the soft thersholding method was applied to select the highest FFT coefficients, these coefficients are used in IMF reconstruction, and finally we have obtained the denoised signal by adding the different denoised IMFs. Fig.12 shows the time domain of the IMF1 and the denoised IMF1 which correspond to the signal of the last day. To display the difference between the raw signals and the de-noised signals using DEEMDFFT method and as the Kurtosis (Ku) is an indicator used for the detection of the impulses, the kurtosis

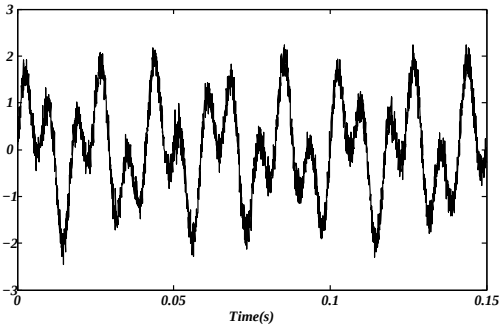

Figure 4: The noisy simulated signal.

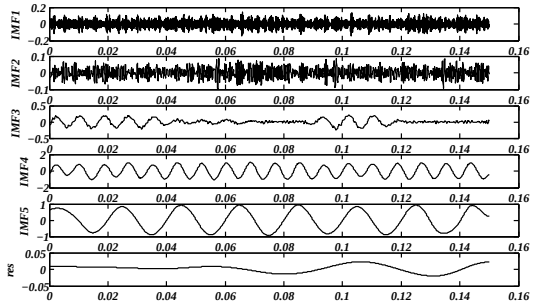

Figure 5: EEMD decomposition of the noisy signal.

values were calculated from day 2 to day 13 (table 4), for the raw signals and for the de-noised signals based on (DEEMDFFT) method.

Day	Observations	Day	Observations
2	First day of acquisition, not of anomaly	8	No evolution tooth 1/2 no evolution
3	No anomaly	9	Tooth 1/2 no evolution , Tooth 15/16 beginning of chipping
4	////	10	Evolution of chipping tooth 15/16
5	////	11	////
6	////	12	////
7	Chipping tooth 1/2	13	Chipping over all the width of tooth 15/16

Table 3: Expert report

6 Discussion and conclusion

Fig.13 shows clearly that the Kurtosis values of raw signals increase rapidly after day 11, which indicates development of the fault, but before that the variation of the Kurtosis values are arbitraries Fig.14. However, the Kurtosis values of the de-noised signals starts increasing in a uniform way from the seventh day which indicates that the fault appears on gear from the seventh day.The results presented in this study demonstrate that the combination method of EEMD and denoising based on FFT can be used to identify early damage in gear boxes. We note that the proper choice of the thersholding parameters in the post processing stage is important. Numerical results prove that the de-noising method (DEEMDFFT) can increase the precision of results given by the two methods EEMD and denoising based on FFT. This method is very simple, does not require any choice of wavelet or the scale and it is capable of reducing noise and preserving signal information.

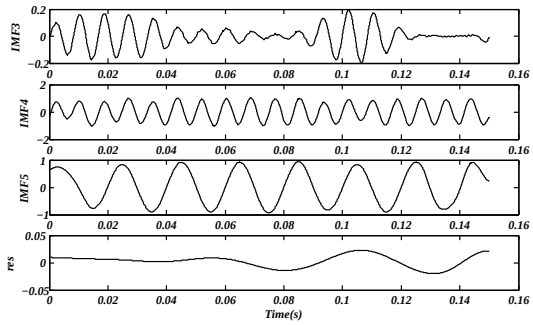

Figure 6: The denoised IMFs using the denoising algorithm based on FFT.

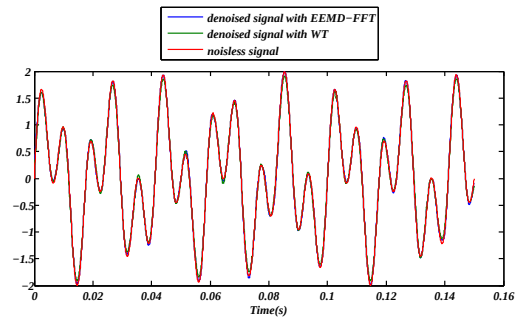

Figure 7: The denoised simulated signal using DEEMDFFT and WT.

References

[1] G. Dalpiaz, A.Rivola, R.Rubini, *Effectiveness and sensitivity of vibration processing techniques for local fault detection in gears*, Mechanical Systems and Signal Processing, Vol. 14, No. 3, (2000), pp. 387-412.

[2] C. M.Harris , A.G.Piersol, *Harris shock and vibration handbook*, in Mcgraw-Hill, editor, *5th ed.*, (2002) .

[3] P.D.McFadden, *Detecting fatigue cracks in gears by amplitude and phase demodulation of the meshing vibration*, Transaction of the ASME, Journal of Vibration , Acoustics, stress and Reability, in design vol.108, (1986), pp.165-170.

[4] R.B.Randall, *Cepstrum analysis and gearbox fault detection*, Technical Report 13-150, Bruel Kjaer Technical Review, (1981), Denmark.

[5] B.D.Forrester, *Use of Wigner Ville distribution in helicopter transmission fault detection*, in iProc of the Australian, symposium on Signal Processing and Applications, ASSPA89, Adelaide, Australia, 17-19. April 1989, pp.77-82.

[6] W. J.Staszewski, *Local tooth fault detection in gear boxes using a moving window procedure*, Mechanical Systems and Signal Processing, Vol 11, No3, (1997), pp.331-350.

[7] W.J.Wang , P.D. Mcfadden, *Application of orthogonal wavelet to early gear damage detection*, Mechanical Systems and Signal Processing, 9(5),(1997) pp.497-507.

[8] C.Capdessus, M.Sidahmed, *Cyclostationary processes application in gear faults early diagnosis*, Mechanical Systems and Signal Processing, 14(3),(2000), pp. 371-685.

[9] L.Cohen, *Time-frequency distributions a review*, Proceedings of the IEEE 77 (7), (1989), pp.941-981.

[10] G. Svend, K.G.Hansen, *The analysis of nonstationary signals*, Journal of Sound and Vibration,(1997), pp.40-46.

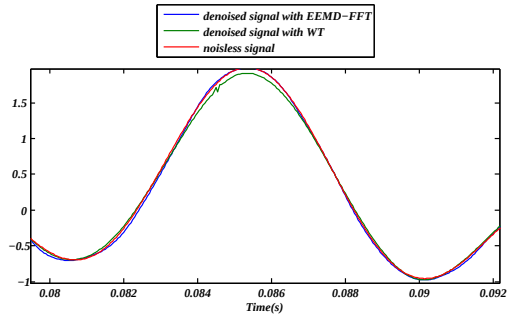

Figure 8: The zoom of Fig.7.

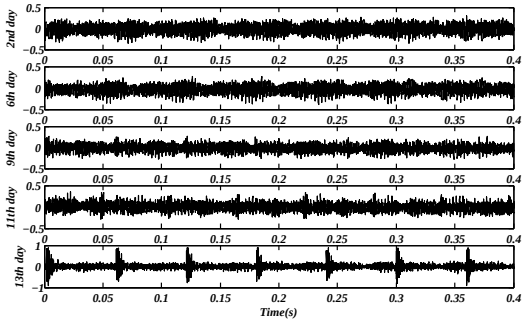

Figure 9: The acceleration signals in time domain.

[11] I.Daubechies, *Ten lectures on wavelets* , Philadelphia, society for industrial and applied Mathematics (SIAM) 1992. 357 p. ISBN 0898712742.

[12] S.J.Loutridis, *Damage detection in gear systems using empirical mode decomposition*, Engineering Structures vol. 26, pp.1833-1841.

[13] N. E. Huang, Z Shen, . and S. R. Long, (1998). *The empirical mode decomposition and the Hilbert spectrum for nonlinear and non-stationary time series analysis*, in: Proceedings of the Royal Society of London Series, 454, pp. 903-995.

[14] N. E. Huang, Z.Shen, and S. R. Long, (1999). *A new view of nonlinear water waves: the Hilbert spectrum*, Annual Review of Fluid Mechanics , vol 31, pp. 417-457.

[15] J.S.Cheng, D.J.Yu, J.S. Tang, (2008). *Application of frequency family separation method based upon EMD and local Hilbert energy spectrum method to gear fault diagnosis*, Mechanism and Machine Theory, vol 43, pp.712-723.

[16] Liu, B. Riemenschneider, S. and Xub, Y. (2005). Gearbox fault diagnosis using empirical mode decomposition and Hilbert spectrum, Mechanical Systems and Signal Processing 17(9), p. 1-17

[17] Gao, Q., Duan, C., Fan, H., Meng, Q. (2008). Rotating machine fault diagnosis using empirical mode decomposition, Mechanical Systems and Signal Processing (22) p.1072-1081.

[18] N.E.Huang, M.L.Wu, and S. R. Long, (2003). *A confidence limit for the empirical mode decomposition and Hilbert spectral analysis*, Proceedings of the Royal Society of London (459) pp.2317-2345.

[19] Z.Wu , N.E.Huang, (2009). *Ensemble empirical mode decomposition: a noise-assisted data analysis method, advances in adaptive data analysis*, vol. 1, no. 1, pp.1-41 c world scientific publishing company.

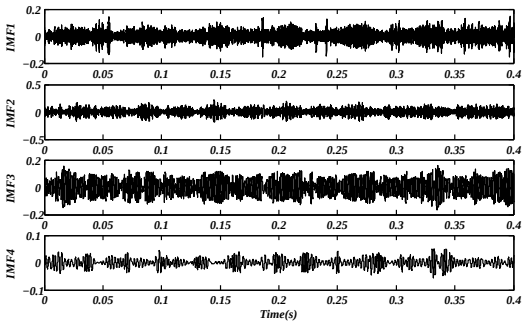

Figure 10: EEMD of signal of second day.

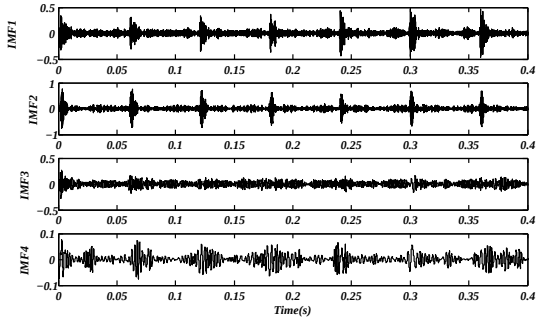

Figure 11: EEMD of signal of the last day.

[20] H. Mahgoun, R.E. Bekka, AFelkaoui, . (2012). *Gearbox fault diagnosis using ensemble empirical mode decomposition (EEMD) and residual signal*, Mechanics Industry, Vol. 13, Issue 01, pp.33-44.

[21] D. L. Donoho, (1995). *De-noising by soft-thresholding* , IEEE Trans. on Inf. Theory, 41, 3, pp.613-627.

[22] H. Mahgoun, A. Felkaoui, R.E. Bekka, *The effect of resampling on the analysis results of ensemble empirical mode decomposition (EEMD)*, 6^{th} international conference acoustical and vibratory surveillance methods and diagnostic techniques, Surveillance6 International confrrence, Compiegne, France, October 25-26, 2011.

[23] N. Vlassis, A.Likas, (1999). *A Kurtosis-based dynamic approach to Gaussian mixture modeling*, Man and Cybernetics parts, A29, pp.393-399.

[24] A. Parey, M. El Badaoui, F. Guillet, and N. Tandon, (2006). *Dynamic modelling of spur gear pair and application of empirical mode decomposition-based statistical analysis for early detection of localized tooth defect*, Journal of sound and vibration 294, pp.547-561.

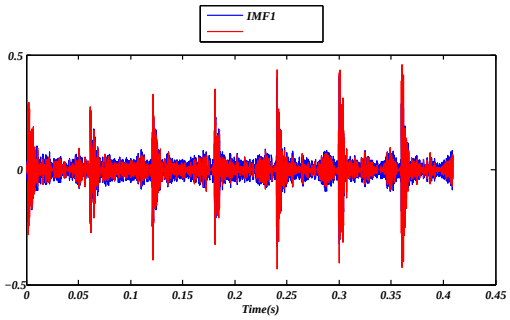

Figure 12: Comparaison between IMF1 and the denoised IMF1of the last day.

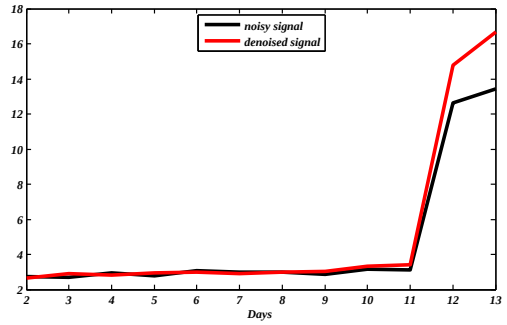

Figure 13: Kurtosis value of the acceleration signal from day 2 to day11 before and after de-noising.

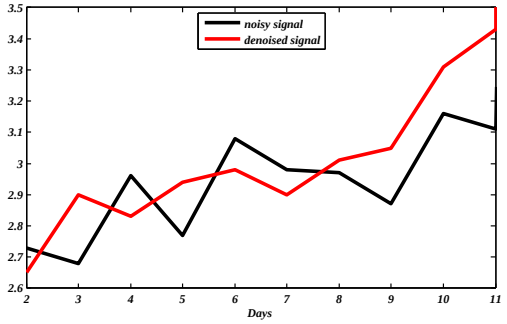

Figure 14: Kurtosis value of the acceleration signal from day 2 to day11 before and after de-noising (Zoomed).

Day	2	3	4	5	6	7
Ku (Raw signal)	2.73	2.68	2.96	2.77	3.08	2.98
Ku (denoised signal) (DEEMDWT)	2.65	2.90	2.83	2.94	2.98	2.90
Day	8	9	10	11	12	13
Ku (Raw signal)	2.97	2.87	3.16	3.11	12.64	13.44
Ku (denoised signal) (DEEMDWT)	3.01	3.05	3.31	3.43	14.78	16.69

Table 4: Kurtosis values of the raw signals and denoised signals using DEEMDFFT.